# New Stationary Frame Transformation for Control of a Three-Phase Power Converter Under Unbalanced Grid Voltage Sags

Grzegorz Iwanski, *Senior Member, IEEE*, Paweł Maciejewski, and Tomasz Łuszczyk

***Abstract*— This article deals with a new nonlinear transformation providing representation of unbalanced three-phase signals (voltage and currents) as vectors that have constant components in a new rotating $d'q'$ frame. Using the proposed transformations, the control system of a power electronic converter operating with an unbalanced grid can be equipped with proportional–integral (PI) controllers, without the use of resonant terms, for which antiwindup structures are more complicated and nonintuitive. This article presents the derivation of new direct and inverse transformations, features, a power converter model in a new frame, simulation results showing the waveforms of signals transformed to the new non-Cartesian frame, and simulation and experimental results of the voltage-oriented control for a grid-connected power converter.**

***Index Terms*— ac–dc power conversion, Clarke's transformation, current control.**

## NOMENCLATURE

| | |
|---|---|
| $x$ | General vector representing any three-phase signal (voltage, current, and possibly flux in an electric machine). |
| $x_a$, $x_b$, and $x_c$ | General three-phase signals. |
| $x_\alpha$ and $x_\beta$ | $\alpha\beta$ components of the general vector in a classic stationary frame obtained by the Clarke transformation. |
| $x'_\alpha$ and $x'_\beta$ | $\alpha\beta$ components of the general vector in a modified non-Cartesian stationary frame obtained with the new transformation. |
| $x'_d$ and $x'_q$ | $dq$ components of the general vector in a modified non-Cartesian rotating frame obtained with the new transformation and Park's rotation transformation. |
| $x^i_\alpha$ and $x^i_\beta$ | $\alpha\beta$ components of the general vector in a classic stationary frame obtained by the inverse new transformation. |
| $\lvert x_a\rvert$, $\lvert x_b\rvert$, and $\lvert x_c\rvert$ | Amplitudes of $abc$ three-phase general signals. |
| $\lvert x_\alpha\rvert$ and $\lvert x_\beta\rvert$ | Amplitudes of classic $\alpha\beta$ stationary frame components of the general vector. |
| $\lvert x'_\alpha\rvert$ and $\lvert x'_\beta\rvert$ | Amplitudes of new non-Cartesian $\alpha\beta$ stationary frame components of the general vector. |
| $\lvert x_{abc}\rvert^{\max}$ | Maximum amplitude from among amplitudes of phase general signals. |
| $\lvert x\rvert_{\text{base}}$ | Base amplitude for the new transformation (base vector length giving the new transformation output signals amplitudes equal to $\lvert x\rvert_{\text{base}}$). |
| $M_\alpha$ and $M_\beta$ | Scaling factors for new $\alpha'\beta'$-axes. |
| $x^d_\alpha$, $x^d_\beta$, $x^q_\alpha$, and $x^q_\beta$ | Direct ($^d$) and quadrature ($^q$) components of general vector $\alpha\beta$ components. |
| $x^d_a$, $x^d_b$, $x^d_c$, $x^q_a$, $x^q_b$, and $x^q_c$ | Direct ($^d$) and quadrature ($^q$) components of general vector three-phase signals. |
| $x_{p\alpha}$ and $x_{p\beta}$ | General vector positive-sequence $\alpha\beta$ components. |
| $x_{n\alpha}$ and $x_{n\beta}$ | General vector negative-sequence $\alpha\beta$ components. |
| $\lvert x_p\rvert$ | Positive-sequence general vector length. |
| $\theta_s$ | Synchronous angle (transformation angle for Park's transformation) calculated on the basis of positive-sequence $\alpha\beta$ fundamental frequency components. |
| $\theta_\alpha$ and $\theta_\beta$ | Angle between $\alpha\beta$ vector components and the positive-sequence vector $\alpha$ component. |
| $\theta_{\beta\alpha}$ | The angle between $\beta$ and $\alpha$ vector components. |
| $u_g$ | Grid voltage vector. |
| $u_c$ | Converter voltage vector. |
| $i$ | Converter current vector. |
| $u_{\text{dc}}$ | DC voltage. |
| $R$ | Grid filter resistance. |
| $L$ | Grid filter inductance. |
| $C_{\text{dc}}$ | DC bus capacitance. |

Manuscript received May 7, 2020; revised June 26, 2020 and July 27, 2020; accepted July 27, 2020. Date of publication July 30, 2020; date of current version July 30, 2021. The work was supported by the National Science Centre under project Number 2016/23/B/ST7/03942. Recommended for publication by Associate Editor Joseph O. Ojo. *(Corresponding author: Grzegorz Iwanski.)*

The authors are with the Institute of Control and Industrial Electronics, Warsaw University of Technology, Warszawa 00-662, Poland (e-mail: iwanskig@isep.pw.edu.pl).

Color versions of one or more figures in this article are available at https://doi.org/10.1109/JESTPE.2020.3012971.

Digital Object Identifier 10.1109/JESTPE.2020.3012971

| | |
|---|---|
| $\omega_s$ | Synchronous pulsation (fundamental frequency positive-sequence components pulsation). |
| $\mathbf{T}_{\boldsymbol{\alpha'\beta'}}$ | New transformation from classic $\alpha\beta$ stationary frame to the new $\alpha'\beta'$ stationary frame. |
| $\mathbf{T}_{\mathbf{d'q'}}$ | Classic Park's transformation from the new $\alpha'\beta'$ stationary frame to the new rotating $d'q'$ frame. |
| $\mathbf{T}^{-\mathbf{1}}_{\boldsymbol{\alpha'\beta'}}$ | Inverse transformation from the new $\alpha'\beta'$ stationary frame to the classic $\alpha\beta$ stationary frame. |
| $p$ | Instantaneous power $p$ component (by Akagi). |
| $p_{\text{avg}}$ | Average value of instantaneous $p$ power component (definitional active power). |
| $\lvert i\rvert^{\text{max\_ref}}$ | Reference value of phase current maximum amplitude (reference current limit). |
| outRi$_d$ and outRi$_q$ | Output signals of current vector components regulators. |
| $(^*)$ | Reference signals for dc voltage controller and converter current controllers. |
| LPF | Low-pass filter. |
| HPF | High-pass filter. |
| BSF | Band-stop filter. |
| SVM | Space vector modulator. |
| SOGI | Second-order generalized integrator. |

## I. Introduction

POWER electronic three-phase converters used as grid interfaces (see Fig. 1) enable negative-sequence management, impossible in passive rectifiers or in electric machines operated when directly connected to the power grid. Interconnection requirements called grid codes are more and more restrictive. Some of the newest standards require the assistance of converter-based energy conversion systems during voltage sags, including management of negative sequence during asymmetrical sags, to improve stability of the power system and increase the quality of delivered energy [1].

Positive- and negative-sequence decomposition-based control methods are the most popular for negative-sequence management. The methods use separate coordinates frames and proportional–integral (PI) current regulators for each sequence [2]. Recently, proportional–resonant (PR) controllers in the *abc* frame [3], in a stationary frame [4], [5], or PI–resonant (PIR) controllers in a rotating frame [6] are applied, but still with sequences decomposition. One can find methods of reference signals calculation matching the desired control targets, without sequences decomposition [7], [8]. Regardless of the selected target, resonant terms are still used to track the reference current including a 50-Hz frequency component if controlled in the stationary $\alpha\beta$ frame or constant and a 100-Hz component if controlled in a rotating synchronously $dq$ reference frame.

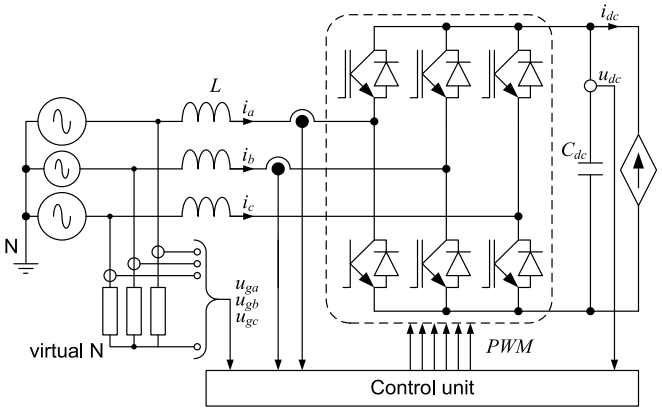


Fig. 1. Scheme of the power circuit of a three-phase power electronic converter operating with an unbalanced grid voltage.

Although the digital implementation of resonant terms as a regulator is not complicated when some rules are kept (e.g., prewarping in discretization [9]), the whole structure does not include only pure resonant terms. The associated structures responsible for state limitation of the term (antiwindup) are more complicated than in PI controllers and not intuitive.

Simple cutting of oscillatory signals [10] makes the signals no longer sinusoidal. Proper antiwindup for oscillatory terms needs the introduction of an oscillatory terms damping factor when the control signal exceeds the limit [11]. Change in the damping factor is based on an additional controller (e.g., proportional controller with a high gain or integral) responsible for limitation of the resonant term output signal.

An additional term limiting the control signal, influencing the damping factor, requires an additional tuning procedure, and due to the strong nonlinearity of such a structure, tuning (selection of gains) is not a trivial problem to be done optimally. Thus, optimization methods, such as linear-quadratic LQ [12], or more advanced, such as particle swarm [13], are used. They require powerful software for solving the Riccati equation for LQ optimization or particle swarm optimization run. Such software is common in large industrial companies but not in small and medium firms.

When resonant terms operate in parallel to the other terms (such as integral terms in the PIR regulator in control realized in a rotating frame), antiwindup structures are even more complex because more than one term requires state limitation (resonant and integral) separately, and the level of signals from both terms should be selected depending on total control signal limitation. This is not a trivial case, especially when more than one variable is under control [14], as it is in the case of a three-phase power converter. This problem is simpler to solve (it is intuitive) for a classic PI controller.

The problem is a minor issue in double-synchronous reference frame-based methods that use PI controllers. Knowing the value of reference current in each of the four axes ($dq$-axes for positive and $dq$-axes for negative sequence) and the model of the converter, the components of control signals can be

assigned and limitations set arbitrarily even with some margin without deterioration of converter properties.

The double-synchronous reference frame-based control method simplifies the issue of current controllers' state limitation and simultaneous control of signal limitation. However, another issue—limitation of total reference converter current at an appropriate level—has to be solved, which is rarely described in the literature for unbalanced current targets. The simplest way is to introduce the limit of the current vector maximum length, which, for the unbalanced current target, equals the sum of positive- and negative-sequence vectors lengths. However, this way of current limitation is not equivalent to the limitation of the phase current amplitude for each type of asymmetry [8]. Thus, more sophisticated methods are applied, which require more calculations [8], [15].

Independent of the current limitation, a double-synchronous reference frame requires notch filters to avoid mutual interactions between positive- and negative-sequence control paths, which worsens the dynamics of the control plant seen by the current control loop. This is why more sophisticated current control loops with decoupling terms between positive- and negative-sequence control paths [16] are developed. The improved structures of the double-synchronous reference frame control still require sophisticated structures of precise limitation of phase current, but what is more important is a significant number of trigonometric function calculations for rotation transformation in the main paths and in decoupling paths.

This article presents a new approach of three-phase power converter control based on transformation to the non-Cartesian frame. The aim is to find new frames in which controlled variables in the rotating frame during an asymmetrical voltage dip and/or asymmetrical reference current are constant regardless of the fact whether the reference current asymmetry has asymmetry corresponding to the voltage asymmetry, opposite asymmetry, or it is symmetrical.

New transformation parameters are determined by finding the amplitude and phase of voltage components in a natural $\alpha\beta$ frame and adaptation of parameters to match a new reference, which can be a sinusoidal current with asymmetry corresponding to or opposite to the grid voltage asymmetry or no asymmetry. By choosing different combinations of the calculated amplitude multipliers and phase shifts, the selected control objectives can be achieved.

Modified transformations are known also in the postfault operation of multiphase machines [17] or even in three-phase machines fed from four-wire power converters [18] in which new reference frames can be calculated offline for each phase fault and mapped in a table due to the fixed position of stator phase windings. For a grid-connected converter, the estimation of new transformation parameters has to be done online because, during a voltage dip, phase displacement and voltage drop depend on the type and depth of grid voltage dip.

To find online new transformation parameters, a combination of second-order LPF and HPF was chosen as a phasor estimator because of its convergence speed and low computational intensity.

## II. Derivation of the Proposed Transformation

### A. Direct Transformation

For the three-wire system with no zero-sequence component, Clarke's transformation [19] described by

$$\begin{bmatrix} x_\alpha \\ x_\beta \end{bmatrix} = \begin{bmatrix} 1 & 0 & 0 \\ 0 & \frac{\sqrt{3}}{3} & -\frac{\sqrt{3}}{3} \end{bmatrix} \begin{bmatrix} x_a \\ x_b \\ x_c \end{bmatrix} \tag{1}$$

is used to represent three-phase signals $x_a$, $x_b$, and $x_c$ by two orthogonal components $x_\alpha$ and $x_\beta$ of the vector in a stationary frame. As the transformation can be applied for different variables, such as three-phase voltage, three-phase current, or three-phase flux (in an electric machine), in this section, the theory will be explained using general variable $x$, which can represent any of the mentioned variables.

The $x_\alpha$ and $x_\beta$ components of vector $x$ containing positive and negative sequences can be described by

$$x_\alpha = |x_\alpha| \cos(\theta_s - \theta_\alpha) \tag{2a}$$

$$x_\beta = |x_\beta| \cos\big(\theta_s - \theta_\beta\big) \tag{2b}$$

in which $|x_\alpha|$ and $|x_\beta|$ are components amplitudes, and $\theta_\alpha$ and $\theta_\beta$ are phase shifts between $\alpha\beta$ components and positive-sequence $\alpha$ component.

Park's transformation [20] allows the representation of vector $x$ by constant components in a rotating frame. When an imbalance occurs, both instantaneous angular speed $\omega$ of vector rotation and vector length $|x|$ contain grid voltage double-frequency oscillations. Thus, to eliminate the influence of negative sequence on control, the $dq$ frame rotates synchronously with a positive-sequence vector, and the synchronous angular speed $\omega_s$ is obtained using different structures of phase-locked loops (PLLs). When negative sequence occurs, components amplitudes $|x_\alpha|$ and $|x_\beta|$ differ, or/and the phase shift between $\alpha\beta$ components $\theta_{\beta\alpha} = \theta_\beta - \theta_\alpha$ differs from $\pi/2$. Then, $x_d$ and $x_q$ components contain double-grid-frequency oscillatory terms that, when controlled, require more sophisticated methods than simple PI controllers.

The theoretical approach proposed in this article introduces an additional transformation between the stationary $\alpha\beta$ frame and the rotating $dq$ frame. Therefore, the final obtained variables are constant (do not contain oscillatory terms).

Let us assume that there exists a nonlinear transformation to the new stationary $\alpha'\beta'$ frame providing new components $x'_\alpha$ and $x'_\beta$ with the same amplitudes $|x|_{\text{base}}$ and synchronized with the positive-sequence $\alpha\beta$ components of vector $x$. The new components $x'_\alpha$ and $x'_\beta$ are described by

$$x'_\alpha = |x|_{\text{base}} \cos\theta_s \tag{3a}$$

$$x'_\beta = |x|_{\text{base}} \sin\theta_s \tag{3b}$$

in which the new amplitude $|x|_{\text{base}}$ equal to some reference value will be explained later.

The transformation takes the general form

$$\begin{bmatrix} x'_\alpha \\ x'_\beta \end{bmatrix} = \mathbf{T}_{\boldsymbol{\alpha'\beta'}} \begin{bmatrix} x_\alpha \\ x_\beta \end{bmatrix} = \begin{bmatrix} a & b \\ c & d \end{bmatrix} \begin{bmatrix} x_\alpha \\ x_\beta \end{bmatrix}. \tag{4}$$

There exists an infinite number of $a - b$ and $c - d$ pairs that meet condition (2). However, taking into account

that (2) and (3) are time-dependent (because $\theta_s$ is time-dependent), finding the transformation of the time-independent factors $abcd$ for a given asymmetry of the original vector $x$ can be done using two selected conditions (two different $\theta_s$'s) as follows:

$$\left.\begin{aligned} |x|_{\text{base}} &= a|x_\alpha|\cos\theta_\alpha + b|x_\beta|\cos\theta_\beta \\ 0 &= c|x_\alpha|\cos\theta_\alpha + d|x_\beta|\cos\theta_\beta \end{aligned}\right|_{\theta_s=0} \tag{5a}$$

$$\left.\begin{aligned} 0 &= a|x_\alpha|\sin\theta_\alpha + b|x_\beta|\sin\theta_\beta \\ |x|_{\text{base}} &= c|x_\alpha|\sin\theta_\alpha + d|x_\beta|\sin\theta_\beta \end{aligned}\right|_{\theta_s=\pi/2}. \tag{5b}$$

From (5a) and (5b) in a simple way, time-independent $abcd$ factors can be derived, and (4) can be written as

$$\boxed{\begin{bmatrix} x'_\alpha \\ x'_\beta \end{bmatrix} = \frac{1}{\sin\theta_{\beta\alpha}} \begin{bmatrix} M_\alpha \sin\theta_\beta & -M_\beta \sin\theta_\alpha \\ -M_\alpha \cos\theta_\beta & M_\beta \cos\theta_\alpha \end{bmatrix} \begin{bmatrix} x_\alpha \\ x_\beta \end{bmatrix}} \tag{6}$$

where

$$\begin{bmatrix} M_\alpha & M_\beta \end{bmatrix} = \begin{bmatrix} \frac{|x|_{\text{base}}}{|x_\alpha|} & \frac{|x|_{\text{base}}}{|x_\beta|} \end{bmatrix}. \tag{7}$$

One of the ways of finding $|x|_{\text{base}}$ is to keep amplitudes $|x'_\alpha|$ and $|x'_\beta|$ equal to the highest phase signals amplitudes $|x_a|, |x_b|, |x_c|$ [see (8)]. Using this factor, we can obtain the unbalanced vector representation as a balanced one with the vector length equal to the maximum from among amplitudes of the three-phase signals. This is helpful in the current vector limitation if we wish not to exceed the assumed maximum amplitude of the current in any phase when the new transformation is used for unbalanced current vector representation

$$|x|_{\text{base}} = \max\{|x_a|, |x_b|, |x_c|\} = |x_{abc}|^{\max}. \tag{8}$$

To bring the vector to the frame rotating with synchronous speed, Park's rotation transformation is used. Both transformations result in. (9)

$$\boxed{\begin{bmatrix} x'_d \\ x'_q \end{bmatrix} = \frac{1}{\sin\theta_{\beta\alpha}} \begin{bmatrix} \cos\theta_s & \sin\theta_s \\ -\sin\theta_s & \cos\theta_s \end{bmatrix} \begin{bmatrix} M_\alpha \sin\theta_\beta & -M_\beta \sin\theta_\alpha \\ -M_\alpha \cos\theta_\beta & M_\beta \cos\theta_\alpha \end{bmatrix} \begin{bmatrix} x_\alpha \\ x_\beta \end{bmatrix}.} \tag{9}$$

Using (2), (7), and (9), it can be proved that $x'_d$ and $x'_q$ components do not have oscillatory terms, and what is more

$$x'_d = |x|_{\text{base}} \tag{10a}$$

$$x'_q = 0 \tag{10b}$$

when the $d'q'$ frame is adequately synchronized. The full derivation of (10ab) is provided in (34) and (35ab).

### *B. Inverse Transformation*

Let us write the transformation (6) as

$$kx'_{\alpha\beta} = \mathbf{T}_{\boldsymbol{\alpha'\beta'}} x_{\alpha\beta} \tag{11}$$

where $k = \sin(\theta_{\beta\alpha})$, and $\mathbf{T}_{\boldsymbol{\alpha'\beta'}}$ is a transformation matrix.

Wishing to find $x^i_{\alpha\beta}$ when $x'_{\alpha\beta}$ is known we can write

$$x^i_{\alpha\beta} = k\mathbf{T}^{-\mathbf{1}}_{\boldsymbol{\alpha'\beta'}} x'_{\alpha\beta'} \tag{12}$$

where $x^i_{\alpha\beta}$ is the vector obtained by the inverse transformation from the new $\alpha'\beta'$ frame to the natural $\alpha\beta$ frame, and

$$\mathbf{T}^{-\mathbf{1}}_{\boldsymbol{\alpha'\beta'}} = \frac{1}{\det\left(\mathbf{T}_{\boldsymbol{\alpha'\beta'}}\right)} \mathbf{C}^{\mathbf{T}} \tag{13}$$

where $\mathbf{C}^{\mathbf{T}}$ is a transposed matrix of complements.

The final form of the inverse transformation from non-Cartesian $\alpha'\beta'$ to the natural $\alpha\beta$ frame can be written as

$$\boxed{\begin{bmatrix} x^i_\alpha \\ x^i_\beta \end{bmatrix} = \begin{bmatrix} \frac{1}{M_\alpha}\cos\theta_\alpha & \frac{1}{M_\alpha}\sin\theta_\alpha \\ \frac{1}{M_\beta}\cos\theta_\beta & \frac{1}{M_\beta}\sin\theta_\beta \end{bmatrix} \begin{bmatrix} x'_\alpha \\ x'_\beta \end{bmatrix}.} \tag{14}$$

Transformation of the $x'$ vector represented in the $d'q'$ frame to the natural $\alpha\beta$ needs two transformations—inverse Park's transformation from the $d'q'$ frame to non-Cartesian $\alpha'\beta'$ and next from non-Cartesian $\alpha'\beta'$ to natural $\alpha\beta$, as follows:

$$\boxed{\begin{bmatrix} x^i_\alpha \\ x^i_\beta \end{bmatrix} = \begin{bmatrix} \frac{1}{M_\alpha}\cos\theta_\alpha & \frac{1}{M_\alpha}\sin\theta_\alpha \\ \frac{1}{M_\beta}\cos\theta_\beta & \frac{1}{M_\beta}\sin\theta_\beta \end{bmatrix} \begin{bmatrix} \cos\theta_s & -\sin\theta_s \\ \sin\theta_s & \cos\theta_s \end{bmatrix} \begin{bmatrix} x'_d \\ x'_q \end{bmatrix}.} \tag{15}$$

### *C. Assignment of Transformation Parameters*

In order to apply the proposed transformation, the amplitudes and phase angles of vector components are needed. Different structures, such as SOGI [21], can be applied to find direct $x^d$ and quadrature $x^q$ fundamental frequency components of the $\alpha\beta$ signals. More effective elimination of harmonics from the grid voltage signals and possible constant component originating from grid voltage sensors offsets can be obtained by a combination of the second-order bandpass filter and LPF [8]. The trigonometric functions of transformation angles can be calculated using the cross and dot products of adequate vectors

$$\sin\theta_\alpha = \frac{x_{p\beta}x^d_\alpha - x_{p\alpha}x^q_\alpha}{|x_\alpha||x_p|} \tag{16a}$$

$$\cos\theta_\alpha = \frac{x^d_\alpha x_{p\alpha} + x^q_\alpha x_{p\beta}}{|x_\alpha||x_p|} \tag{16b}$$

$$\sin\theta_\beta = \frac{x_{p\beta}x^d_\beta - x_{p\alpha}x^q_\beta}{|x_\beta||x_p|} \tag{16c}$$

$$\cos\theta_\beta = \frac{x^d_\beta x_{p\alpha} + x^q_\beta x_{p\beta}}{|x_\beta||x_p|} \tag{16d}$$

$$\sin\theta_{\beta\alpha} = \frac{x^d_\beta x^q_\alpha - x^d_\alpha x^q_\beta}{|x_\alpha||x_\beta|} \tag{16e}$$

$$\sin\theta_s = \frac{x_{p\beta}}{|x_p|} \tag{16f}$$

$$\cos\theta_s = \frac{x_{p\alpha}}{|x_p|}. \tag{16g}$$

Amplitudes $|x_a|, |x_b|$, and $|x_c|$ needed to find $|x|_{\text{base}}$ in (8) can be assigned using inverse Clarke's transformation of $x^d_\alpha, x^q_\alpha$ and $x^d_\beta, x^q_\beta$ to obtain direct and quadrature-phase

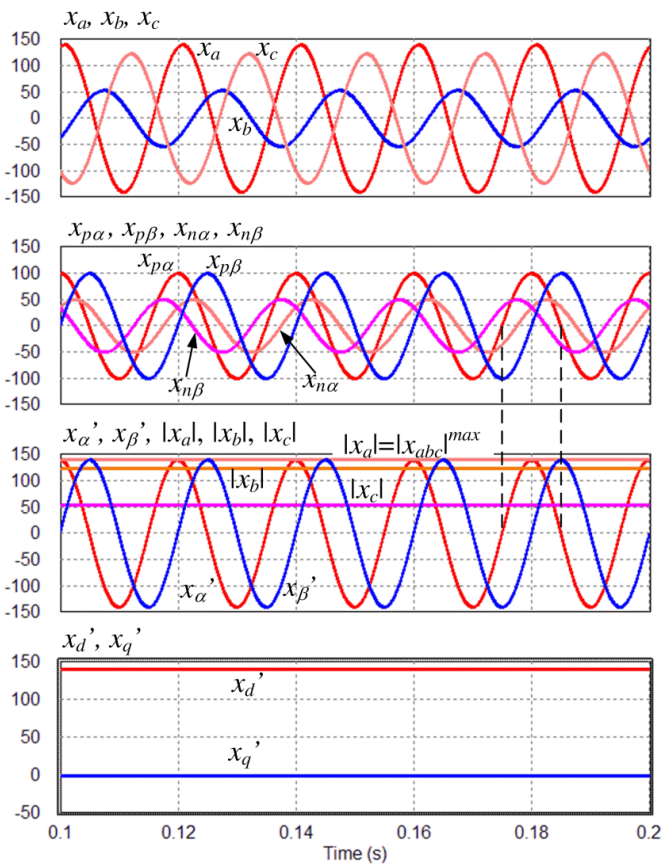


Fig. 2. Example case results of the new transformation from $\alpha\beta$ to $\alpha'\beta'$ frame.

signals $x_a^d, x_a^q$, $x_b^d, x_b^q$, and $x_c^d, x_c^q$, respectively. Furthermore, the amplitudes of phase signals are calculated by

$$|x_a| = \sqrt{\left(x_a^d\right)^2 + \left(x_a^q\right)^2}$$
$$|x_b| = \sqrt{\left(x_b^d\right)^2 + \left(x_b^q\right)^2}$$
$$|x_c| = \sqrt{\left(x_c^d\right)^2 + \left(x_c^q\right)^2}. \tag{17}$$

### D. Example Case Study

Some example case results of the transformation are shown in Fig. 2. The positive-sequence vector length $|x_p|$ equals 100, and the negative-sequence vector length $|x_n|$ equals 50. The equivalent vector maximum length equals the sum of both (150), which is higher than the maximum amplitude of phase signals. Using the new transformation, the $\alpha'\beta'$ vector components have the same phase as $\alpha\beta$ positive-sequence vector components, respectively. The new $\alpha'\beta'$ components have the same amplitude equal to the maximum amplitude from among all three-phase signals. $x_d'$ equals the maximal amplitude as well, whereas $x_q'$ equals zero.

### E. Transformation Parameters for Opposite Asymmetry

In the inverter mode, the converter current asymmetry opposite to grid voltage asymmetry may be beneficial for the grid as it can reduce the grid voltage imbalance factor at the point of common coupling due to the different voltage increase on the grid impedance in each phase [8]. If we wish to implement the new transformations for such a case (opposite asymmetry of current in relation to the voltage asymmetry), some additional analysis is needed.

To achieve constant vector components representing opposite asymmetry of three-phase signals in a new rotating frame and keeping (10ab), the parameters of the new $\alpha\beta/\alpha'\beta'$ transformation have to be calculated on the basis of $\alpha\beta$ components representing opposite asymmetry of three-phase signals. Opposite asymmetry is represented by the new $\alpha\beta$ components meeting the conditions (18ab), in which new $\alpha\beta$ components representing the opposite asymmetry are related to the original $\alpha\beta$ components.

$$x_\alpha = -x_\beta\left(t - \frac{T}{4}\right) \tag{18a}$$
$$x_\beta = x_\alpha\left(t - \frac{T}{4}\right). \tag{18b}$$

It can be checked by making $xy$ plots of $x_\alpha = f(x_\beta)$ for the original components and the recalculated components [see (18ab)] and observing that orientations of both hodographs are opposite. Taking into account (18ab), further derivation can be made for recalculated direct and quadrature $\alpha\beta$ components of vector $x$ for the representation of opposite asymmetry

$$x_{g\alpha}^d = -x_{g\beta}^d\left(t - \frac{T}{4}\right) = -x_{g\beta}^q \tag{19a}$$
$$x_{g\alpha}^q = -x_{g\beta}^q\left(t - \frac{T}{4}\right) = x_{g\beta}^d \tag{19b}$$
$$x_{g\beta}^d = x_{g\alpha}^d\left(t - \frac{T}{4}\right) = x_{g\alpha}^q \tag{19c}$$
$$x_{g\beta}^q = x_{g\alpha}^q\left(t - \frac{T}{4}\right) = -x_{g\alpha}^d. \tag{19d}$$

Finally, the transformation parameters, such as $|x|_{\text{base}}$, calculated on the basis of (8) and (17), and trigonometric functions, calculated with (16a)–(16g), are determined using (19a)–(19d) in the case in which the desired asymmetry of converter current is opposite to the asymmetry of grid voltage. Fig. 3 shows original three-phase signals $x_a, x_b$, and $x_c$, the original $x_\alpha$ and $x_\beta$ and new $x_\alpha$ and $x_\beta$ signals for the opposite asymmetry, $x_d'$ and $x_q'$, in a rotating frame for opposite asymmetry, and, finally, $x_a, x_b$, and $x_c$ phase signals representing opposite asymmetry obtained by inverse transformation with parameters calculated using (19a)–(19d).

### F. Practical Implementation of Transformations

This article shows how to avoid the calculation of trigonometric functions to reduce the computational burden of the microcontroller. All trigonometric functions are calculated exactly as it is presented in (16a)–(16g) and used in the new transformation (16a)–(16e) as well as in the Park transformation (16f) and (16g), i.e., as cross and dot products of the extracted $\alpha\beta$ components of the grid voltage vector (for finding new transformation parameters) and $\alpha\beta$ components of the positive-sequence grid voltage vector (for finding the Park transformation parameters).

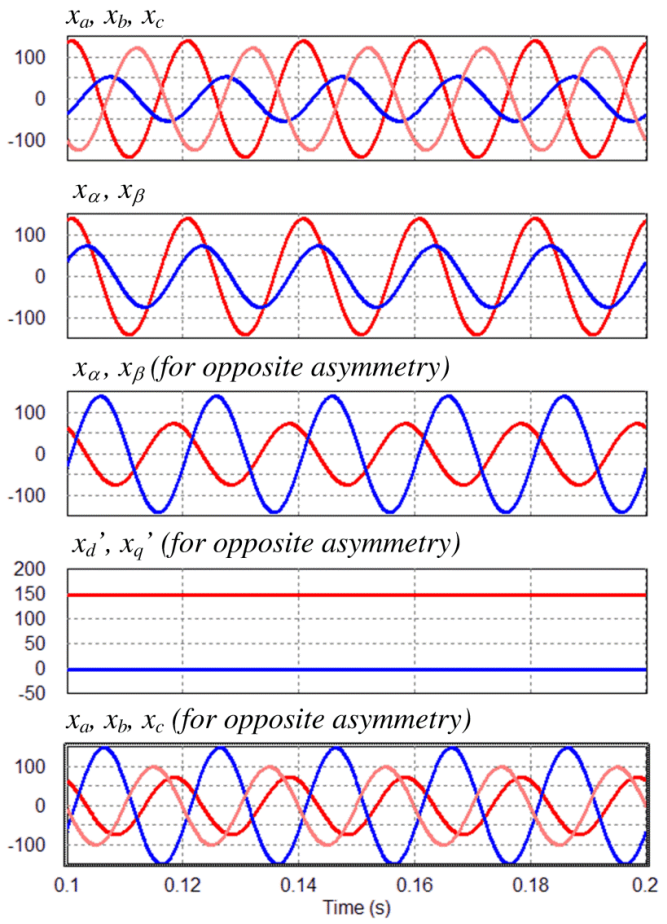


Fig. 3. Example case results of the new transformation from $\alpha\beta$ to $\alpha'\beta'$ frame for the opposite asymmetry signal representation.

Several signals are needed, such as direct $\alpha\beta$ components, quadrature $\alpha\beta$ components (signals shifted by $\pi/2$ to the direct components), and positive-sequence $\alpha\beta$ components of the grid voltage, and the set of low- and high-pass digital filters is used to extract them. Digital filter functions are something structurally (in terms of hardware structure) supported by digital signal processors.

Using (16a)–(16e), the proposed transformation can be derived in the following form without the use of trigonometric functions, and even the number of divisions (which takes some number of computational cycles) is reduced to one calculation (division) only:

$$\begin{bmatrix} x'_\alpha \\ x'_\beta \end{bmatrix} = \frac{|x|_{\text{base}}}{|x_p|\left(x^d_\beta x^q_\alpha - x^d_\alpha x^q_\beta\right)} \times \begin{bmatrix} x_{p\beta}x^d_\beta - x_{p\alpha}x^q_\beta & -x^d_\beta x_{p\alpha} + x^q_\beta x_{p\beta} \\ -x_{p\beta}x^d_\alpha - x_{p\alpha}x^q_\alpha & x^d_\alpha x_{p\alpha} + x^q_\alpha x_{p\beta} \end{bmatrix} \begin{bmatrix} x_\alpha \\ x_\beta \end{bmatrix}. \tag{20}$$

However, this is a technical manner, which does not change a new theoretical approach.

What is more, in the experimental tests, the TMS320F28335 DSP processor was used, but the newest versions of DSP microcontrollers from the same C2000 family, such as TMS320F28377 or TMS320F28379, are supported with hardware trigonometric math units (TMUs), significantly reducing computational burden for such type of functions, so even using the fundamental equations presented in this article, calculation of trigonometric functions is not a problem. Similarly, for division operation and other more complicated algebraic operations (such as calculation of square root), a floating-point unit (FPU) can be involved, which significantly shortens the time of the calculation process. The price of these newest computational units is not significantly higher than the commonly used TMS320F28335. There are other benefits of the newest DSP models from the same family, such as better precision of ADC converters or dual-core (in some models), and possibly in newly developed industrial power converters, new control units will replace older ones. The rest of the calculations are simple algebraic functions. The most demanding is four times the calculated square root, but it takes less computational time than a trigonometric function.

Similarly, the Park transformation without intermediate calculation of trigonometric functions can be derived as

$$\begin{bmatrix} x'_d \\ x'_q \end{bmatrix} = \frac{1}{|x_p|} \begin{bmatrix} x_{p\alpha} & x_{p\beta} \\ -x_{p\beta} & x_{p\alpha} \end{bmatrix} \begin{bmatrix} x'_\alpha \\ x'_\beta \end{bmatrix} \tag{21}$$

with the use of (16f) and (16g).

The new transformation can be combined with the Clarke transformation to one form. Taking into account that for the three-wire system, the discussion neglects the zero-sequence component that we are controlling a 2-D vector (a three-phase three-wire system). The zero-sequence component is not measured (in a three-wire system, the converter current naturally does not contain zero sequence, whereas, in the measured grid voltage, zero sequence is eliminated by measurement of the phase voltage related to the virtual neutral point (see Fig. 1) and not to the neutral wire that is missing). For such a case, we can describe the Clarke and new transformations in one form

$$\begin{aligned} \begin{bmatrix} x'_\alpha \\ x'_\beta \end{bmatrix} &= \frac{1}{\sin\theta_{\beta\alpha}} \begin{bmatrix} M_\alpha \sin\theta_\beta & -M_\beta \sin\theta_\alpha \\ -M_\alpha \cos\theta_\beta & M_\beta \cos\theta_\alpha \end{bmatrix} \begin{bmatrix} 1 & 0 & 0 \\ 0 & \frac{\sqrt{3}}{3} & -\frac{\sqrt{3}}{3} \end{bmatrix} \begin{bmatrix} x_a \\ x_b \\ x_c \end{bmatrix} \\ &= \frac{1}{\sin\theta_{\beta\alpha}} \begin{bmatrix} M_\alpha \sin\theta_\beta & -\frac{\sqrt{3}M_\beta}{3}\sin\theta_\alpha & \frac{\sqrt{3}M_\beta}{3}\sin\theta_\alpha \\ -M_\alpha \cos\theta_\beta & \frac{\sqrt{3}M_\beta}{3}\cos\theta_\alpha & -\frac{\sqrt{3}M_\beta}{3}\cos\theta_\alpha \end{bmatrix} \\ &\quad \times \begin{bmatrix} x_a \\ x_b \\ x_c \end{bmatrix}. \end{aligned} \tag{22}$$

However, these are only mathematical derivations, and from the point of view of the presented concept, it introduces nothing. If we add to this form to Park's rotation transformation, nothing will be simplified, but the calculation will increase the computational burden.

The Park transformation can be used in the form

$$x_d = \frac{2}{3}\left(x_a \cos\theta_s + x_b \cos\left(\theta_s - \frac{2}{3}\pi\right) + x_c \cos\left(\theta_s + \frac{2}{3}\pi\right)\right) \tag{23a}$$

$$x_q = \frac{2}{3}\left(x_a \sin\theta_s + x_b \sin\left(\theta_s - \frac{2}{3}\pi\right) + x_c \sin\left(\theta_s + \frac{2}{3}\pi\right)\right) \tag{23b}$$

allowing the transformation of signals from *abc* to *dq* frame directly. Such a manner takes more computational cycles because even if we have $\sin\theta_s$ and $\cos\theta_s$ directly from PLL, other trigonometric functions must be calculated in a classic way, which means that, first, $\theta_s$ is calculated using $tg^{-1}$ and, later, they are calculated functions $\cos(\theta_s - (2/3)\pi)$, $\cos(\theta_s + (2/3)\pi)$, $\sin(\theta_s - (2/3)\pi)$, and $\sin(\theta_s + (2/3)\pi)$. To avoid these calculations, additional filters must be used, which will shift sine and cosine functions from PLL by 120°, which is generally possible, but not comfortable. As we know and can easily design and implement the filters that introduce phase shift exactly equal to 90°, filters shifting exactly by –120° and +120° (or –240) are unusual (but not impossible).

Filters introducing phase shift +120° (or –240°) are more problematic. In the case of +120°, the filter should be at least second order and have high passing character, which means it will gain harmonics. The filter shifting −240° must be at least the third order. This is why in practical implementation, it is easier to transform the variables subsequently, first from *abc* to $\alpha\beta$ and next from $\alpha\beta$ to the rotating *dq* frame.

From this point of view, the use of combined transformation from *abc* to the $d'q'$ frame transformation is neither simpler nor comfortable, so it is recommended to use cascaded sets of transformations from *abc* to $\alpha\beta$, next from $\alpha\beta$ to $\alpha'\beta'$, and finally from $\alpha'\beta'$ to $d'q'$ to eliminate problematic computation of trigonometric functions.

## III. Control Method Using the New Transformations

### A. Model of a Grid Converter in a New Frame

The classic equation of a grid-connected power converter in a stationary $\alpha\beta$ frame is described by

$$u_{c\alpha\beta} = Ri_{\alpha\beta} + L\frac{di_{\alpha\beta}}{dt} + u_{g\alpha\beta} \tag{24}$$

whereas, using the transformation (6), we can obtain

$$\mathbf{T}_{\boldsymbol{\alpha'\beta'}} u_{c\alpha\beta} = R\mathbf{T}_{\boldsymbol{\alpha'\beta'}} i_{\alpha\beta} + L\mathbf{T}_{\boldsymbol{\alpha'\beta'}}\frac{di_{\alpha\beta}}{dt} + \mathbf{T}_{\boldsymbol{\alpha'\beta'}} u_{g\alpha\beta} \tag{25}$$

identical to

$$u'_{c\alpha\beta} = Ri'_{\alpha\beta} + L\frac{di'_{\alpha\beta}}{dt} + u'_{g\alpha\beta}. \tag{26}$$

The parameters of transformation (6) are time-independent, so there is no influence of transformation on the current time derivative other than the current vector transformation.

Rotation transformation from the $\alpha'\beta'$ to *dq* frame is identical to the classic rotation transformation from $\alpha\beta$ to *dq*; thus, the converter model in a new $d'q'$ frame is presented as

$$\mathbf{T}_{\mathbf{d'q'}} u'_{c\alpha\beta} = R\mathbf{T}_{\mathbf{d'q'}} i'_{\alpha\beta} + L\mathbf{T}_{\mathbf{d'q'}}\frac{di'_{\alpha\beta}}{dt} + \mathbf{T}_{\mathbf{d'q'}} u'_{g\alpha\beta}. \tag{27}$$

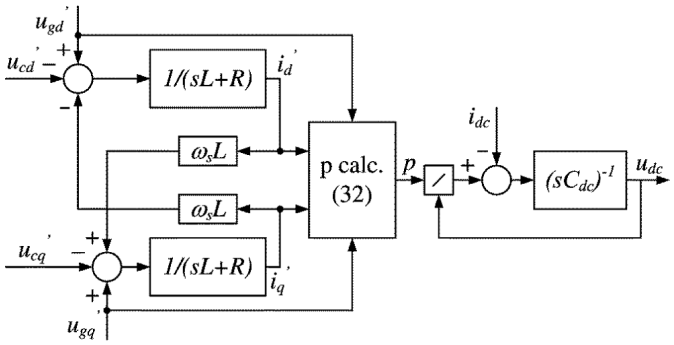


Fig. 4. Model of the power converter in a non-Cartesian rotating frame.

Finally

$$u'_{cdq} = \left(Ri'_{dq} + L\frac{di'_{dq}}{dt}\right) + j\omega_s Li'_{dq} + u'_{gdq} \tag{28}$$

where the term in parentheses represents a control plant, $j\omega_s Li'_{dq}$ represents the coupling terms, and $u_{g\alpha\beta}$ is the disturbance.

The dc bus voltage derivative

$$\frac{du_{\mathrm{dc}}}{dt} = \frac{1}{C_{\mathrm{dc}}}\left(\frac{p}{u_{\mathrm{dc}}} - i_{\mathrm{dc}}\right) \tag{29}$$

depends on the *p* component of instantaneous power and dc bus current $i_{\mathrm{dc}}$.

The *p* component of instantaneous power can be calculated in a classic way by

$$p = \frac{3}{2}\left(u_{g\alpha} i_{g\alpha} + u_{g\beta} i_{g\beta}\right). \tag{30}$$

Taking into consideration transformations (6) and (14), the *p* power component (30) can be further derived as

$$p = \frac{3}{2}\left(\frac{1}{M_\alpha}\cos(\theta_s - \theta_\alpha)u'_{gd} i_\alpha + \frac{1}{M_\beta}\cos\left(\theta_s - \theta_\beta\right)u'_{gd} i_\beta\right) \tag{31}$$

through the replacement of voltage $u_{g\alpha\beta}$ components by $u'_{gdq}$ components and next as

$$\begin{aligned} p = \frac{3}{2}\Bigg(&\frac{1}{M_\alpha^2}\left(\frac{1}{2} + \frac{\cos 2(\theta_s - \theta_\alpha)}{2}\right)u'_{gd} i'_d - \frac{1}{M_\alpha^2}\frac{\sin 2(\theta_s - \theta_\alpha)}{2}u'_{gd} i'_q \\ &+ \frac{1}{M_\beta^2}\left(\frac{1}{2} + \frac{\cos 2\left(\theta_s - \theta_\beta\right)}{2}\right)u'_{gd} i'_d \\ &- \frac{1}{M_\beta^2}\frac{\sin 2\left(\theta_s - \theta_\beta\right)}{2}u'_{gd} i'_q\Bigg) \end{aligned} \tag{32}$$

through the replacement of the current $i_{\alpha\beta}$ components by $i'_{dq}$ components. The terms connected with $u'_{gq}$ in the rotating frame synchronized with the $u'_g$ space vector equal zero. The full derivation of the instantaneous *p* power component is shown in (36a) and (36b).

A model of the power converter in a new rotating frame is shown in Fig. 4 with the neglected power losses on inductor resistance and power semiconductors. An average value of the *p* power component $p_{\mathrm{avg}}$ (definitional active power *P*), which

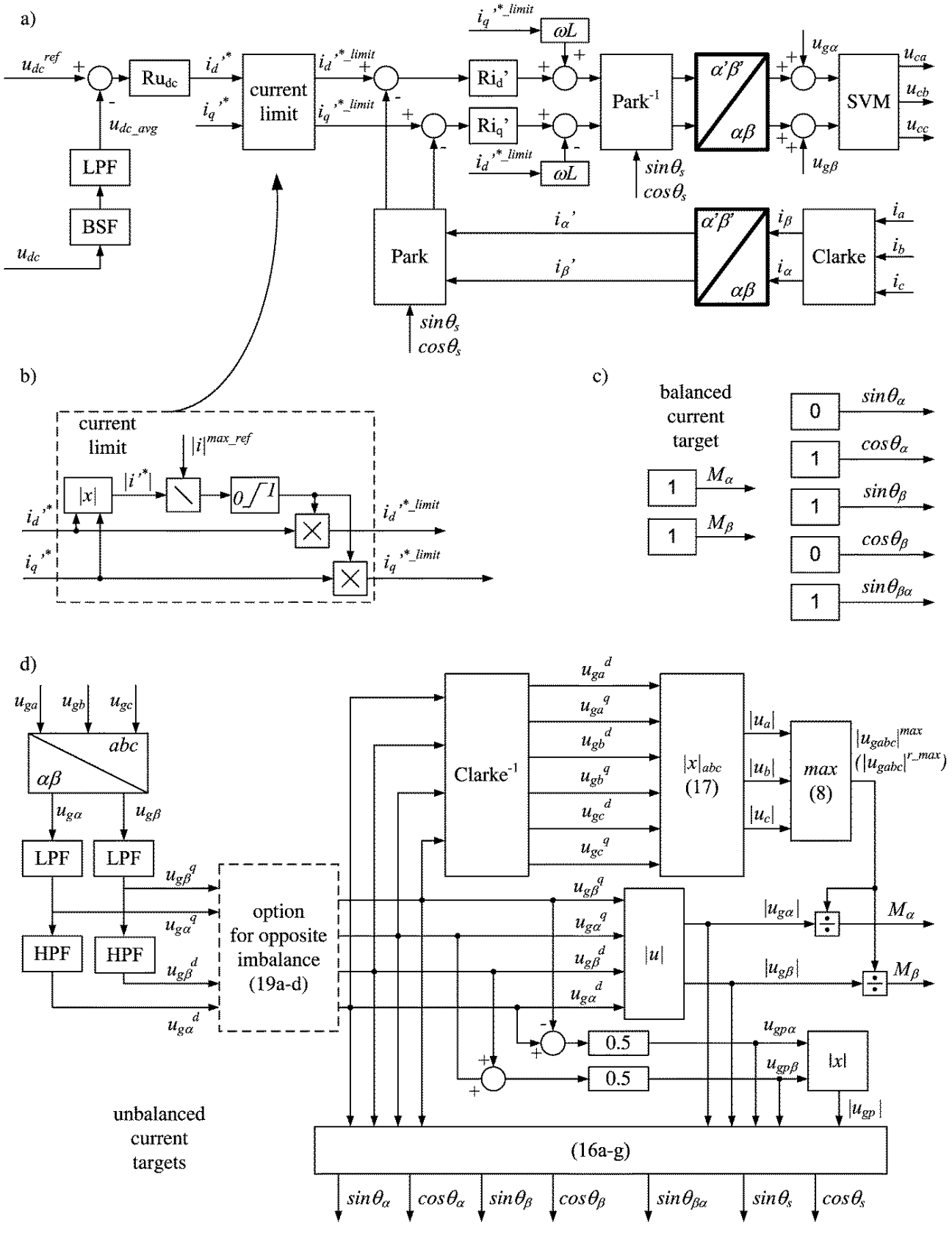


Fig. 5. Proposed control method and the method of calculation of the non-Cartesian frame transformation parameters. (a) Main structure of voltage-oriented control with the new transformations. (b) Example method of reference current limitation. (c) Set of transformation parameters for the balanced current target. (d) Method of transformation parameters' calculation for corresponding and (optionally) opposite current asymmetry.

is responsible for energy transfer between the power grid and dc bus, equals

$$p_{\text{avg}}=\frac{3}{4}\left(\frac{1}{M_\alpha^2}+\frac{1}{M_\beta^2}\right)u'_{gd}i'_d=\frac{3\left(|u_{g\alpha}|^2+|u_{g\beta}|^2\right)}{4\left(|u_{gabc}|^{\max}\right)^2}u'_{gd}i'_d. \quad (33)$$

Taking into account that $u'_{gd}$ is constant for a given grid voltage asymmetry, the average value of power $p_{\text{avg}}$ depends only on the $i'_d$ component of the converter current space vector. Thus, the dc bus voltage controller can directly reference the $i'_d$ component of the converter current space vector.

A similar derivation can be made for the $q$ power component, the average value $q_{\text{avg}}$ of which depends on the $i'_q$ component of the converter current space vector.

### *B. Scheme of Voltage-Vector-Oriented Control Using the New Transformations*

A control system allowing three main targets of the converter current vector analyzed in the literature is shown in Fig. 5. Fig. 5(a) shows the main structure of voltage-oriented control with the new transformation. Fig. 5(b) shows the method of current limitation. This is an example solution, in which the $d$ and $q$ components of the reference current are limited proportionally. However, different solutions are possible in which priority is set for the $d$ component (responsible for active power) or the $q$ component (responsible for reactive power). However, this is not the main focus of this article. Fig. 5(c) shows an arbitrary set of transformation parameters for a symmetrical sinusoidal current target. This way, the new transformation changes nothing similar to the opposite $\alpha'\beta'$ to $\alpha\beta$ transformation. We can totally resign from the $\alpha\beta$ to $\alpha'\beta'$ transformation and opposite $\alpha'\beta'$ to $\alpha\beta$ for this target but leaving these transformations in the control structure simplifies the implementation of the control code in the microcontroller. Fig. 5(d) shows the details of transformation parameters determination for two targets of unbalanced current vector—with asymmetry corresponding to voltage asymmetry and optionally with asymmetry opposite to voltage asymmetry. The block named "option for opposite imbalance" is for the converter current opposite asymmetry target only.

## IV. Simulation Results of Control Methods With Non-Cartesian Frame Transformation

### *A. Simulation Results for Current Control Targets*

Simulation tests have been made at positive-sequence voltage $|u_p| = 260$ V, negative-sequence voltage $|u_n| = 65$ V, and the maximum amplitude from among all phase voltages amplitudes $|u_{abc}|^{\max} = 325$ V. Two targets (reference current corresponding to or opposite to asymmetry) have been shown as most interesting and not typically applied in practice.

Simulation tests have been made without $\text{Ru}_{\text{dc}}$ controllers with arbitrarily referenced current vector components in a modified $d'q'$ reference frame ($i_d^{'*}$ step from 0 to 10 A in 0.04s and $i_q^{'*}$ step from 0 to −5 A in 0.08 s). Switching frequency equals 10 kHz, the dc bus voltage is 600 V, the filter inductance is 4 mH, and the inductor resistance is 0.1 Ω.

To obtain reasonably good results of reference current tracking, the current controllers must be strong enough. Particularly, the gain of the controller should provide a good enough dynamic of the closed-loop system. However, this issue is independent of the transformation used because transformation parameters are calculated only on the basis of the grid voltage signal and without the use of any controlled variables (converter current or dc voltage) neither the output signals of the controllers.

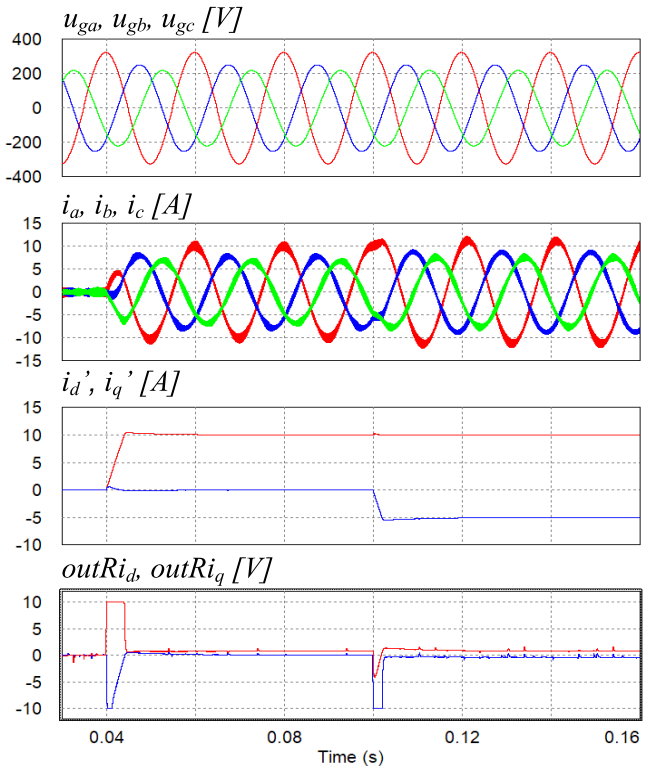


Fig. 6. Simulation results presenting unbalanced grid voltages $u_{ga}$, $u_{gb}$, and $u_{gc}$, unbalanced converter currents $i_a$, $i_b$, and $i_c$, converter current vector components in a modified $d'q'$ rotating frames $i'_d$ and $i'_q$, and output signals of controllers *outPId* and *outPIq* for current asymmetry corresponding to the voltage asymmetry.

Responses for current controllers gain equal to 10 (see Fig. 6) and 2 (see Fig. 7) are shown. Selected PI current controller time constant $T_i$ equals 0.04 s in both cases. Some differences in transient response are visible, but the steady-state values are obtained at the same level in both cases due to an integral part of controllers. The transient response difference depending on the controller's parameters is something natural, but, due to the fact that transformation parameters are calculated on the basis of grid voltage signals, no influence of the regulator parameters on the transformation is observed.

Fig. 8 presents the case with converter current asymmetry opposite to the grid voltage asymmetry chosen. In both cases, due to adequately matched transformation parameters, current components in a new rotating $d'q'$ coordinates are constant in steady states, so as to output signals of the PI controllers despite converter current asymmetry. Fig. 9 presents the case with a symmetrical sinusoidal current target for identical conditions of grid voltage imbalance and reference signals of current vector components.

Fig. 10 shows the simulation results of converter operation with asymmetrical grid voltage sag (25% of asymmetry

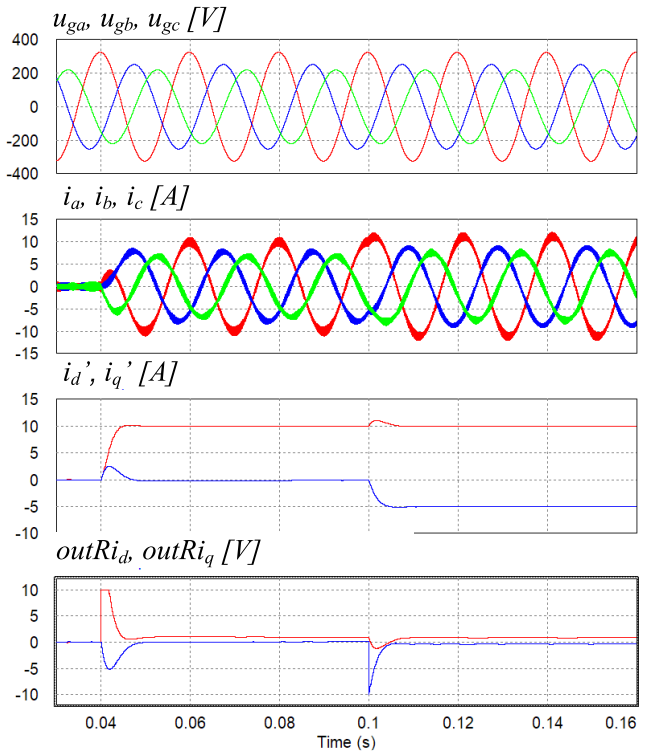


Fig. 7. Simulation results of rotating frame control with the proposed new transformation to the non-Cartesian frame.

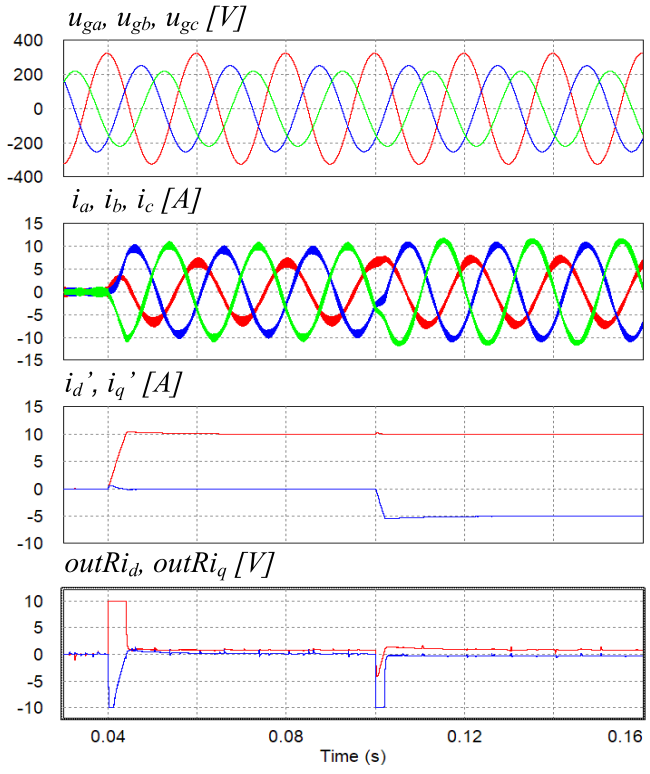


Fig. 8. Simulation results presenting unbalanced grid voltages $u_{ga}$, $u_{gb}$, and $u_{gc}$, unbalanced converter currents $i_a$, $i_b$, and $i_c$, converter current vector components in a modified $d'q'$ rotating frames $i'_d$ and $i'_q$, and output signals of controllers *outPId* and *outPIq*, for the current asymmetry opposite to the voltage asymmetry.

calculated as a ratio of negative-sequence vector length to the positive-sequence vector length) with current asymmetry

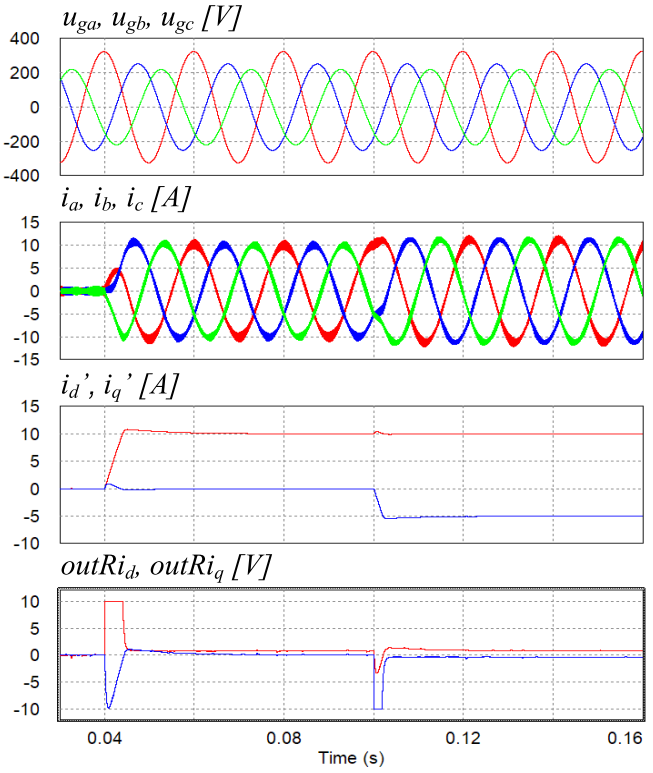


Fig. 9. Simulation results presenting unbalanced grid voltages $u_{ga}$, $u_{gb}$, and $u_{gc}$, unbalanced converter currents $i_a$, $i_b$, and $i_c$, converter current vector components in a modified $d'q'$ rotating frames $i'_d$ and $i'_q$, and output signals of controllers *outPId* and *outPIq*, for the symmetrical sinusoidal current target.

opposite to the voltage asymmetry during the voltage sag and with a symmetrical current at the symmetrical grid voltage. It can be seen that the converter phase currents' amplitudes during sag do not exceed the amplitude of the symmetrical current.

Output signals of the current vector components regulators are disturbed in transient states due to the change of transformation parameters that are found over a time period. The shortening of this transient may be obtained by more sophisticated and faster filtration than used in this article. However, faster methods of filtration are more complex, whereas the obtained current quality is satisfactory.

### *B. Comparison With Stationary Frame Control and Double-Synchronous Reference Frame Control*

The example comparative test is related to the converter current with imbalance corresponding to the imbalance of grid voltage (see Figs. 11–13). The methods taken into consideration are the double-synchronous reference frame DSRF controls with the measured signals' decomposition. The decomposition uses band-stop filters BSF to eliminate double-grid-frequency oscillations in each separate frame. The band-stop filters are seen as additional dynamic terms by current controllers; therefore, current controllers cannot have so high gain as in the case in which only one sample delay exists between the measurement and the control action. This is why, in the step response, the coupling of the control

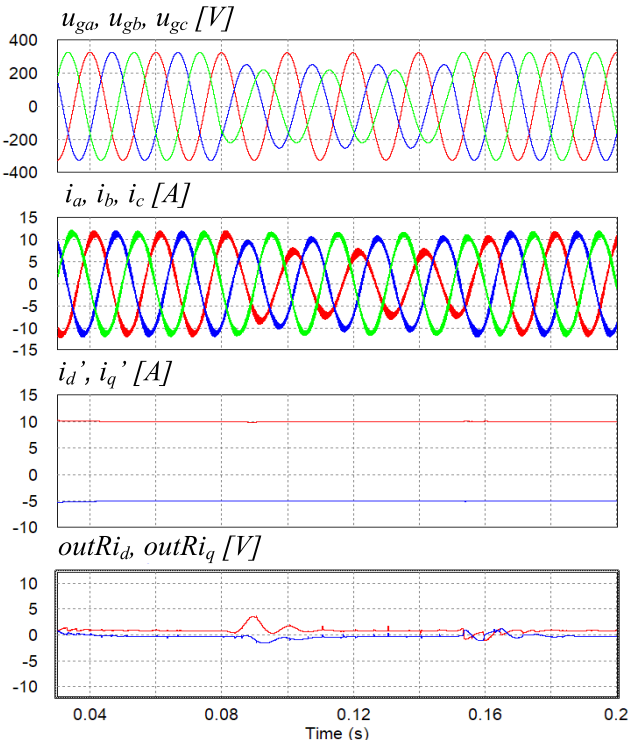


Fig. 10. Simulation results presenting unbalanced grid voltages $u_{ga}$, $u_{gb}$, and $u_{gc}$, unbalanced converter currents $i_a$, $i_b$, and $i_c$, converter current vector components in a modified $d'q'$ rotating frames $i'_d$ and $i'_q$, and output signals of controllers *outPId* and *outPIq*, for current asymmetry opposite to the voltage asymmetry at 25% unbalanced grid voltage dip transient.

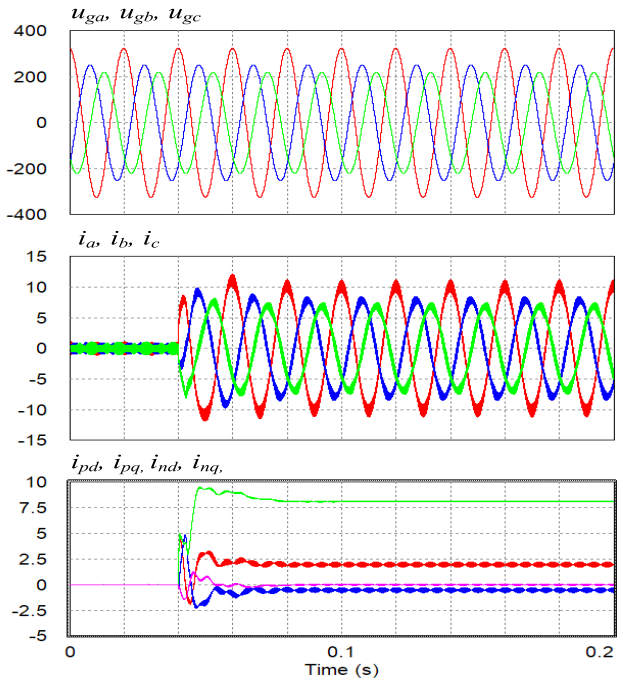


Fig. 11. Simulation results of the double-synchronous reference frame DSRF control with notch filters used for double-grid-frequency oscillations filtration.

axes between $dq$ positive-sequence and $dq$ negative-sequence current vectors components is observed in Fig. 11. Simultaneously, small overregulation of current occurs.

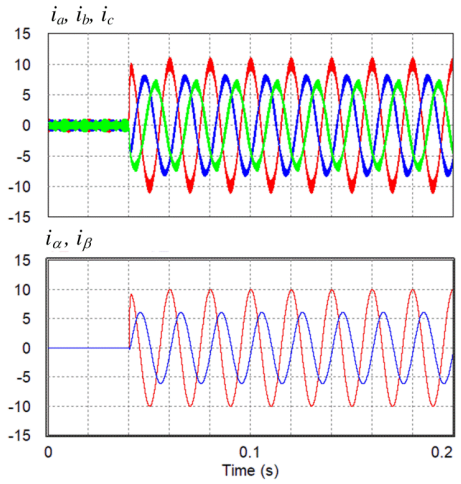


Fig. 12. Simulation results of the stationary frame control with oscillatory terms used in the PR current regulators.

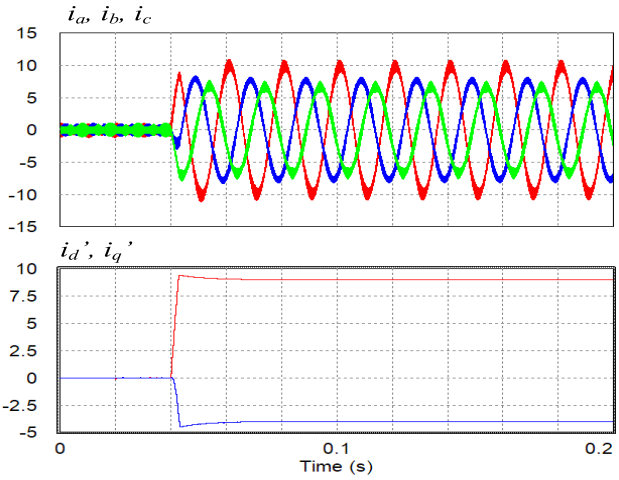


Fig. 13. Simulation results of the rotating frame control with the proposed new transformation to the non-Cartesian frame.

A faster response can be achieved without sequences decomposition using PR controllers in the $\alpha\beta$ frame (see Fig. 12). Current regulators can have high gain due to a lack of additional dynamic terms deteriorating the total dynamics of the control plant. If we wish to have unbalanced current represented in the $\alpha\beta$ frame, one way or another, the positive- and negative-sequence components have to be referenced prior to obtaining common $\alpha\beta$ signals, so the referencing is similar to the DSRF control. In both cases, the true phase current amplitude limitation (which is different than maximal vector length limitation) requires further calculations. This topic is very often neglected in publications although it is crucial from the point of view of converter safety.

## V. Experimental Tests of Control Methods With Non-Cartesian Frame Transformation

Experimental tests were made with a 5.5-kW converter. The converter parameters are provided in Table I. The parameters of filters used in the control algorithm are provided in Table II.

TABLE I
PARAMETERS OF THE POWER CONVERTER USED IN THE LABORATORY

| Symbol | PARAMETER | Value |
|---|---|---|
| $U_{gn}$ | Nominal phase voltage (L-N rms) | 133V |
| $I_n$ | Rated current rms | 14A |
| $L$ | Grid filter inductance | 1.2mH |
| $R_L$ | Inductor resistance | 40mΩ |
| $C_{dc}$ | dc link capacitance | 1mF |
| $f_s$ | Switching frequency | 10kHz |

TABLE II
PARAMETERS OF THE FILTERS

| FILTER | GAIN | CUT-OFF FREQUENCY | DAMPING FACTOR |
|---|---|---|---|
| grid voltage LPF | 1 | 50Hz | 0.5 |
| grid voltage HPF | 1 | 50Hz | 0.5 |
| dc voltage LPF | 1 | 150Hz | $\sqrt{2}$ |
| FILTER | GAIN | CENTER FREQUENCY | STOPPING BAND |
| dc voltage BPF | 1 | 100Hz | 40Hz |

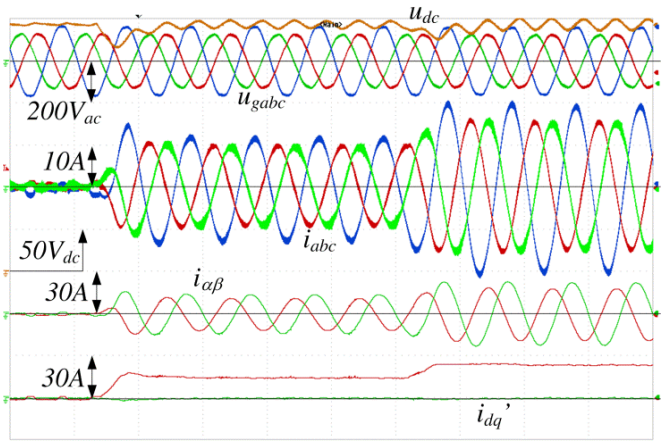


Fig. 14. Experimental test results presenting the grid voltage $u_{gabc}$, converter current $i_{abc}$, current components in the $\alpha\beta$ frame $i_{\alpha\beta}$, and current components in the $d'q'$ frame $i'_{dq}$, for current asymmetry corresponding to the voltage asymmetry.

Figs. 14–16 present the power converter operation in the laboratory setup during grid voltage imbalance and step change of the operating point by the increase of the dc bus load. After the initial no-load operation, a 2-kW resistive load and next additional 1.5-kW resistive load for rectifier operation are applied on the dc side. The selected load represents the maximum possible power in the case of Fig. 14 (current asymmetry corresponding to the voltage asymmetry) without exceeding any phase current constraints (20 A of current amplitude) at given grid voltage imbalance.

Fig. 17 presents the case of the inverter to rectifier change. The opposite current asymmetry target is most beneficial for the grid of the three presented targets, whereas, in the rectifier mode, the corresponding current asymmetry is preferable for the grid because, in the rectifier mode, this target provides

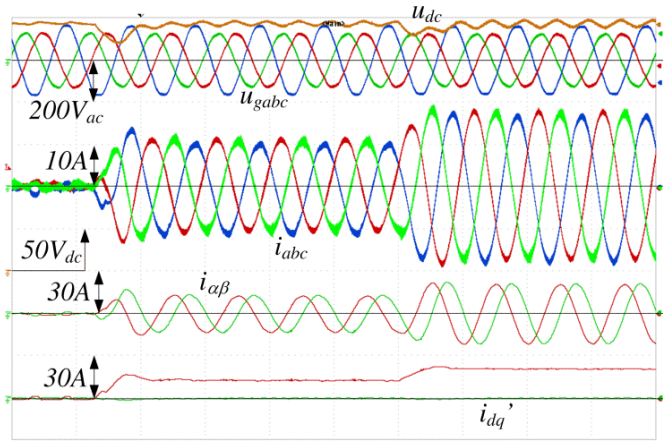


Fig. 15. Experimental test results presenting the grid voltage $u_{gabc}$, converter current $i_{abc}$, current components in the $\alpha\beta$ frame $i_{\alpha\beta}$, and current components in the $d'q'$ frame $i'_{dq}$ for the symmetrical current target.

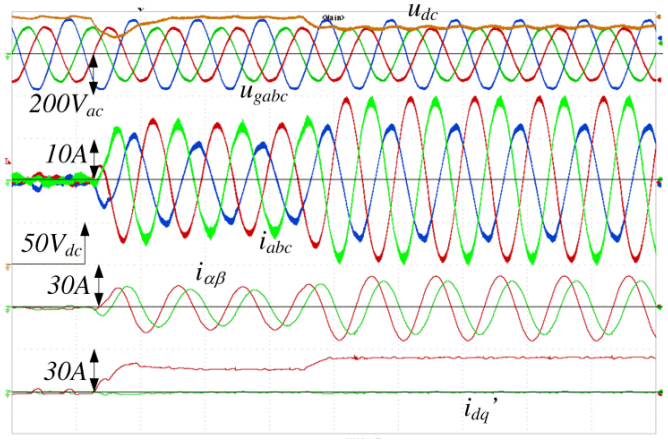


Fig. 16. Experimental test results presenting the grid voltage $u_{gabc}$, converter current $i_{abc}$, current components in $\alpha\beta$ frame $i_{\alpha\beta}$, current components in the $d'q'$ frame $i'_{dq}$, for current asymmetry opposite to the voltage asymmetry.

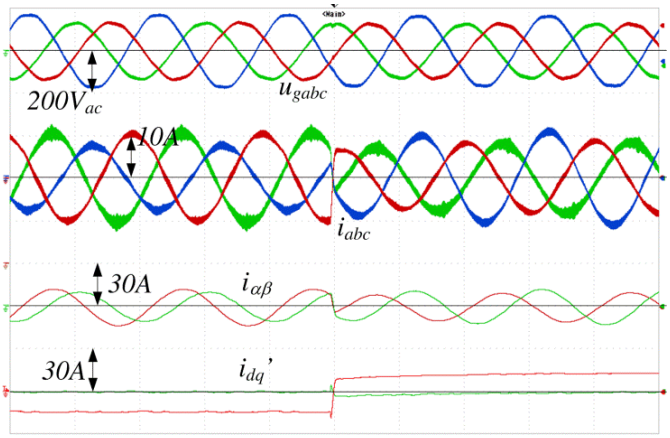


Fig. 17. Experimental test results at the change from the inverter mode with opposite current asymmetry to the rectifier mode with corresponding current asymmetry.

the lowest voltage asymmetry factor when impedance voltage drops are taken into consideration [8]. In some publications,

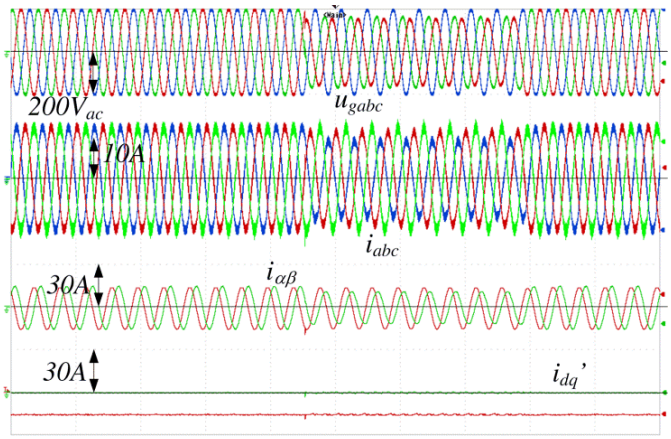


Fig. 18. Experimental test results during an asymmetrical voltage dip in the inverter mode with the opposite current asymmetry.

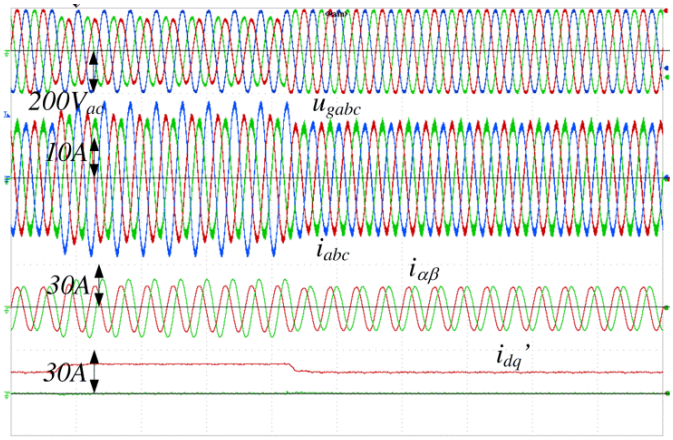


Fig. 19. Experimental test results during an asymmetrical voltage dip in the rectifier mode with the corresponding current asymmetry.

the authors proposed the current opposite asymmetry target also for rectifier operation [22], [23], because, for this target, the $p$ component of instantaneous power is constant, and consequently, no double-grid-frequency dc bus voltage oscillations occur. This is not important in most cases in which the dc bus is used to supply other power electronic converters, such as a machine converter in an electric drive. However, sometimes, the grid power converter directly supplies the load sensitive to voltage changes (e.g., in plasma processes), and in this case, such a target (opposite current asymmetry to the voltage asymmetry) can be of interest also for the rectifier operation mode.

Fig. 18 presents the inverter operation during an asymmetrical voltage dip. For symmetrical grid voltage, converter current becomes symmetrical, whereas, during a sag, the current has opposite asymmetry. In this test, the dc bus voltage is controlled externally, and the current vector components are referenced arbitrarily. It can be seen that, during a sag, the maximum current amplitude equals the amplitude of the balanced current before a sag. Fig. 19 presents a similar transient but for rectifier operation of a converter loaded by 2-kW resistive load and with an enabled dc bus voltage controller.

It can be seen in Fig. 19 that the current amplitude in all phases during the voltage sag is higher than before the sag, to keep the same amount of power for the resistive load. In addition, during this test, the dc load power remained unchanged, so the reference current limitation was disabled so that the current limitation does not exceed current constraints in any phase; except the implementation of the current limitation in the control algorithm, dc load power management should be implemented. In simple words, load power should be reduced to avoid a dc bus voltage drop. Otherwise, the uncontrolled current flow from the grid will occur.

## VI. Conclusion

A new transformation of unbalanced three-phase signals to the non-Cartesian frame in which the new axes positions are matched to three-phase signals imbalance is proposed. As a result, the obtained signals in the new $\alpha'\beta'$ frame are shifted by $\pi/2$. Adequate scaling factors cause that the sinusoidal components have the same amplitudes; therefore, in a new frame, the vector is seen as balanced. A further transformation to the $d'q'$ frame creates constant vector components. The proposed combined transformations from $\alpha\beta$ to $\alpha'\beta'$ and next from $\alpha'\beta'$ to the $d'q'$ frame can be useful in the modification of the voltage-oriented vector control for power converters operating with an unbalanced power grid. Using the proposed transformations, the control variables can be represented by constant components, which makes it possible to eliminate oscillatory terms usually applied in this case as current regulators, for which the antiwindup procedure is not intuitive like for the PI controller. Finding the transformation parameters based on (8), (16), and (17) is relatively simple for application in typical digital signal processing platforms used in the industry. This way of parameters assignment does not

$$\begin{bmatrix} x'_d \\ x'_q \end{bmatrix} = \frac{1}{\sin\theta_{\beta\alpha}} \begin{bmatrix} \cos\theta_s & \sin\theta_s \\ -\sin\theta_s & \cos\theta_s \end{bmatrix} \begin{bmatrix} \frac{|x|_{\text{base}}}{|x_\alpha|}\sin\theta_\beta & -\frac{|x|_{\text{base}}}{|x_\beta|}\sin\theta_\alpha \\ -\frac{|x|_{\text{base}}}{|x_\alpha|}\cos\theta_\beta & \frac{|x|_{\text{base}}}{|x_\beta|}\cos\theta_\alpha \end{bmatrix} \begin{bmatrix} |x_\alpha|\cos(\theta_s-\theta_\alpha) \\ |x_\beta|\cos(\theta_s-\theta_\beta) \end{bmatrix}$$
$$= \frac{|x|_{\text{base}}}{\sin\theta_{\beta\alpha}} \begin{bmatrix} \cos\theta_s\frac{1}{|x_\alpha|}\sin\theta_\beta - \sin\theta_s\frac{1}{|x_\alpha|}\cos\theta_\beta & -\cos\theta_s\frac{1}{|x_\beta|}\sin\theta_\alpha + \sin\theta_s\frac{1}{|x_\beta|}\cos\theta_\alpha \\ -\sin\theta_s\frac{1}{|x_\alpha|}\sin\theta_\beta - \cos\theta_s\frac{1}{|x_\alpha|}\cos\theta_\beta & \sin\theta_s\frac{1}{|x_\beta|}\sin\theta_\alpha + \cos\theta_s\frac{1}{|x_\beta|}\cos\theta_\alpha \end{bmatrix} \begin{bmatrix} |x_\alpha|\cos(\theta_s-\theta_\alpha) \\ |x_\beta|\cos(\theta_s-\theta_\beta) \end{bmatrix} \quad (34)$$

$$
\begin{aligned}
x'_d &= \frac{|x|_{\text{base}}}{\sin\theta_{\beta\alpha}}\big(\cos\theta_s\sin\theta_\beta\cos(\theta_s-\theta_\alpha)-\sin\theta_s\cos\theta_\beta\cos(\theta_s-\theta_\alpha)-\cos\theta_s\sin\theta_\alpha\cos\big(\theta_s-\theta_\beta\big)+\sin\theta_s\cos\theta_\alpha\cos\big(\theta_s-\theta_\beta\big)\big)\\
&= \frac{|x|_{\text{base}}}{\sin\theta_{\beta\alpha}}\big(\cos\theta_s\sin\theta_\beta\cos\theta_s\cos\theta_\alpha+\cos\theta_s\sin\theta_\beta\sin\theta_s\sin\theta_\alpha-\sin\theta_s\cos\theta_\beta\cos\theta_s\cos\theta_\alpha-\sin\theta_s\cos\theta_\beta\sin\theta_s\sin\theta_\alpha\\
&\quad-\cos\theta_s\sin\theta_\alpha\cos\theta_s\cos\theta_\beta-\cos\theta_s\sin\theta_\alpha\sin\theta_s\sin\theta_\beta+\sin\theta_s\cos\theta_\alpha\cos\theta_s\cos\theta_\beta+\sin\theta_s\cos\theta_\alpha\sin\theta_s\sin\theta_\beta\big)\\
&= \frac{|x|_{\text{base}}}{\sin\theta_{\beta\alpha}}\big(\cos^2\theta_s+\sin^2\theta_s\big)\big(\sin\theta_\beta\cos\theta_\alpha-\sin\theta_\alpha\cos\theta_\beta\big)=\frac{|x|_{\text{base}}}{\sin\theta_{\beta\alpha}}\sin\theta_{\beta\alpha}=|x|_{\text{base}} \qquad (35a)\\
x'_q &= \frac{1}{\sin\theta_{\beta\alpha}}\big(-\sin\theta_s\sin\theta_\beta\cos(\theta_s-\theta_\alpha)-\cos\theta_s\cos\theta_\beta\cos(\theta_s-\theta_\alpha)+\sin\theta_s\sin\theta_\alpha\cos\big(\theta_s-\theta_\beta\big)+\cos\theta_s\cos\theta_\alpha\cos\big(\theta_s-\theta_\beta\big)\big)\\
&= \frac{|x|_{\text{base}}}{\sin\theta_{\beta\alpha}}\big(-\sin\theta_s\sin\theta_\beta\cos\theta_s\cos\theta_\alpha-\sin\theta_s\sin\theta_\beta\sin\theta_s\sin\theta_\alpha-\cos\theta_s\cos\theta_\beta\cos\theta_s\cos\theta_\alpha-\cos\theta_s\cos\theta_\beta\sin\theta_s\sin\theta_\alpha\\
&\quad+\sin\theta_s\sin\theta_\alpha\cos\theta_s\cos\theta_\beta+\sin\theta_s\sin\theta_\alpha\sin\theta_s\sin\theta_\beta+\cos\theta_s\cos\theta_\alpha\cos\theta_s\cos\theta_\beta+\cos\theta_s\cos\theta_\alpha\sin\theta_s\sin\theta_\beta\big)=0 \qquad (35b)\\
p &= \frac{3}{2}\left(\left(\frac{1}{M_\alpha}\cos(\theta_\alpha)u'_{g\alpha}+\frac{1}{M_\alpha}\sin(\theta_\alpha)u'_{g\beta}\right)i_\alpha+\left(\frac{1}{M_\beta}\cos\big(\theta_\beta\big)u'_{g\alpha}+\frac{1}{M_\beta}\sin\big(\theta_\beta\big)u'_{g\beta}\right)i_\beta\right)\\
&= \frac{3}{2}\left(\left(\frac{1}{M_\alpha}\cos(\theta_\alpha)\big(\cos(\theta_s)u'_{gd}-\sin(\theta_s)u'_{gq}\big)+\frac{1}{M_\alpha}\sin(\theta_\alpha)\big(\sin(\theta_s)u'_{gd}+\cos(\theta_s)u'_{gq}\big)\right)i_\alpha\right.\\
&\quad\left.+\left(\frac{1}{M_\beta}\cos\big(\theta_\beta\big)\big(\cos(\theta_s)u'_{gd}-\sin(\theta_s)u'_{gq}\big)+\frac{1}{M_\beta}\sin\big(\theta_\beta\big)\big(\sin(\theta_s)u'_{gd}+\cos(\theta_s)u'_{gq}\big)\right)i_\beta\right)\\
&= \frac{3}{2}\left(\frac{1}{M_\alpha}\cos(\theta_s-\theta_\alpha)u'_{gd}i_\alpha+\frac{1}{M_\beta}\cos\big(\theta_s-\theta_\beta\big)u'_{gd}i_\beta\right) \qquad (36a)\\
p &= \frac{3}{2}\left(\frac{1}{M_\alpha}\cos(\theta_s-\theta_\alpha)u'_{gd}\left(\frac{1}{M_\alpha}\cos(\theta_\alpha)i'_\alpha+\frac{1}{M_\alpha}\sin(\theta_\alpha)i'_\beta\right)\right.\\
&\quad\left.+\frac{1}{M_\beta}\cos\big(\theta_s-\theta_\beta\big)u'_{gd}\left(\frac{1}{M_\beta}\cos\big(\theta_\beta\big)i'_{g\alpha}+\frac{1}{M_\beta}\sin\big(\theta_\beta\big)i'_{g\beta}\right)\right)\\
&= \frac{3}{2}\left(\frac{1}{M_\alpha}\cos(\theta_s-\theta_\alpha)u'_{gd}\left(\frac{1}{M_\alpha}\cos(\theta_\alpha)\big(\cos(\theta_s)i'_d-\sin(\theta_s)i'_q\big)+\frac{1}{M_\alpha}\sin(\theta_\alpha)\big(\sin(\theta_s)i'_d+\cos(\theta_s)i'_q\big)\right)\right.\\
&\quad\left.+\frac{1}{M_\beta}\cos\big(\theta_s-\theta_\beta\big)u'_{gd}\left(\frac{1}{M_\beta}\cos\big(\theta_\beta\big)\big(\cos(\theta_s)i'_d-\sin(\theta_s)i'_q\big)+\frac{1}{M_\beta}\sin\big(\theta_\beta\big)\big(\sin(\theta_s)i'_d+\cos(\theta_s)i'_q\big)\right)\right)\\
&= \frac{3}{2}\left(\frac{1}{M_\alpha}\cos(\theta_s-\theta_\alpha)u'_{gd}\left(\frac{1}{M_\alpha}\cos(\theta_s-\theta_\alpha)i'_d-\frac{1}{M_\alpha}\sin(\theta_s-\theta_\alpha)i'_q\right)\right.\\
&\quad\left.+\frac{1}{M_\beta}\cos\big(\theta_s-\theta_\beta\big)u'_{gd}\left(\frac{1}{M_\beta}\cos\big(\theta_s-\theta_\beta\big)i'_d-\frac{1}{M_\beta}\sin\big(\theta_s-\theta_\beta\big)i'_q\right)\right)\\
&= \frac{3}{2}\left(\frac{1}{M_\alpha^2}\left(\frac{1}{2}+\frac{\cos2(\theta_s-\theta_\alpha)}{2}\right)u'_{gd}i'_d-\frac{1}{M_\alpha^2}\frac{\sin2(\theta_s-\theta_\alpha)}{2}u'_{gd}i'_q\right.\\
&\quad\left.+\frac{1}{M_\beta^2}\left(\frac{1}{2}+\frac{\cos2\big(\theta_s-\theta_\beta\big)}{2}\right)u'_{gd}i'_d-\frac{1}{M_\beta^2}\frac{\sin2\big(\theta_s-\theta_\beta\big)}{2}u'_{gd}i'_q\right). \qquad (36b)
\end{aligned}
$$

involve the calculation of trigonometric functions of a high computational burden.

## APPENDIX

See (34), as shown at the bottom of the previous page, and (35)–(36), as shown at the top of the page.

## REFERENCES


[1] *VDE-AR-N 4120: Technical Requirements for the Connection and Operation of Customer Installations to the High-Voltage Network VDE*, Verband der Elektrotechnik, Elektronik und Informationstechnik (VDE), Frankfurt, Germany, Jan. 2015.

[2] M. M. Baggu, B. H. Chowdhury, and J. W. Kimball, "Comparison of advanced control techniques for grid side converter of doubly-fed induction generator back-to-back converters to improve power quality performance during unbalanced voltage dips," *IEEE J. Emerg. Sel. Topics Power Electron.*, vol. 3, no. 2, pp. 516–524, Jun. 2015.

[3] W. Liu, F. Blaabjerg, D. Zhou, and S.-F. Chou, "Modified instantaneous power control with phase compensation and current-limited function under unbalanced grid faults," *IEEE J. Emerg. Sel. Topics Power Electron.*, early access, Mar. 30, 2020, doi: 10.1109/JESTPE.2020.2984475.

[4] Y. Du, X. Lu, H. Tu, J. Wang, and S. Lukic, "Dynamic microgrids with self-organized grid-forming inverters in unbalanced distribution feeders," *IEEE J. Emerg. Sel. Topics Power Electron.*, vol. 8, no. 2, pp. 1097–1107, Jun. 2020.

[5] A. Mora, R. Cardenas, M. Urrutia, M. Espinoza, and M. Diaz, "A vector control strategy to eliminate active power oscillations in four-leg grid-connected converters under unbalanced voltages," *IEEE J. Emerg. Sel. Topics Power Electron.*, vol. 8, no. 2, pp. 1728–1738, Jun. 2020.

[6] X. Guo, Y. Yang, and X. Zhang, "Advanced control of grid-connected current source converter under unbalanced grid voltage conditions," *IEEE Trans. Ind. Electron.*, vol. 65, no. 12, pp. 9225–9233, Dec. 2018.

[7] G. Iwanski, T. Luszczyk, and M. Szypulski, "Virtual-torque-based control of three-phase rectifier under grid imbalance and harmonics," *IEEE Trans. Power Electron.*, vol. 32, no. 9, pp. 6836–6852, Sep. 2017.

[8] G. Iwanski, "Virtual torque and power control of a three-phase converter connected to an unbalanced grid with consideration of converter current constraint and operation mode," *IEEE Trans. Power Electron.*, vol. 34, no. 4, pp. 3804–3818, Apr. 2019.
[9] A. G. Yepes, F. D. Freijedo, O. Lopez, and J. Doval-Gandoy, "High-performance digital resonant controllers implemented with two integrators," *IEEE Trans. Power Electron.*, vol. 26, no. 2, pp. 563–576, Oct. 2011.
[10] M. Rizo, A. Rodriguez, F. J. Rodriguez, E. Bueno, and M. Liserre, "Different approaches of stationary reference frames saturators," in *Proc. 38th Annu. Conf. IEEE Ind. Electron. Soc.*, Oct. 2012, pp. 2245–2250.
[11] A. Galecki, L. Grzesiak, B. Ufnalski, A. Kaszewski, and M. Michalczuk, "Anti-windup strategy for an LQ current controller with oscillatory terms for three-phase grid-tie VSCs in SMES systems," *Power Electron. Drives*, vol. 1, no. 2, 2016, pp. 65–81.
[12] A. Galecki, A. Kaszewski, B. Ufnalski, and L. M. Grzesiak, "State current controller with oscillatory terms for three-level grid-connected PWM rectifiers under distorted grid voltage conditions," in *Proc. 17th Eur. Conf. Power Electron. Appl.*, Sep. 2015, pp. 1–10.
[13] A. Galecki, M. Michalczuk, A. Kaszewski, B. Ufnalski, and L. Grzesiak, "Particle swarm optimization of the multioscillatory LQR for a three-phase grid-tie converter," *Przeglad Elektrotechniczny*, vol. 94, no. 6, 2018, pp. 43–48.
[14] Y. Peng, D. Vraná, R. Hanus, and S. S. R. Weller, "Anti-windup designs for multivariable controllers," *Automatica*, vol. 34, no. 12, pp. 1559–1565, Dec. 1998.
[15] A. Milicua, G. Abad, and M. A. Rodriguez Vidal, "Online reference limitation method of shunt-connected converters to the grid to avoid exceeding voltage and current limits under unbalanced Operation—Part I: Theory," *IEEE Trans. Energy Convers.*, vol. 30, no. 3, pp. 852–863, Sep. 2015.
[16] S. Zhou, J. Liu, L. Zhou, and H. She, "Dual sequence current controller without current sequence decomposition implemented on DSRF for unbalanced grid voltage conditions," in *Proc. IEEE Energy Convers. Congr. Expo. (ECCE)*, Sep. 2014, pp. 60–67.
[17] A. S. Abdel-Khalik, M. S. Hamad, A. M. Massoud, and S. Ahmed, "Postfault operation of a nine-phase six-terminal induction machine under single open-line fault," *IEEE Trans. Ind. Electron.*, vol. 65, no. 2, pp. 1084–1096, Feb. 2018.
[18] X. Zhou, J. Sun, H. Li, and X. Song, "High performance three-phase PMSM open-phase fault-tolerant method based on reference frame transformation," *IEEE Trans. Ind. Electron.*, vol. 66, no. 10, pp. 7571–7580, Oct. 2019.
[19] E. Clarke, *Circuit Analysis of AC Power Systems-Symmetrical and Related Components*, vol. 1. Hoboken, NJ, USA: Wiley, 1943.
[20] R. H. Park, "Two-reaction theory of synchronous machines generalized method of analysis-part i," *Trans. Amer. Inst. Electr. Eng.*, vol. 48, no. 3, pp. 716–727, Jul. 1929.
[21] Z. Xin, X. Wang, Z. Qin, M. Lu, P. C. Loh, and F. Blaabjerg, "An improved second-order generalized integrator based quadrature signal generator," *IEEE Trans. Power Electron.*, vol. 31, no. 12, pp. 8068–8073, Dec. 2016.
[22] L. Hang and M. Zhang, "Constant power control-based strategy for vienna-type rectifiers to expand operating area under severe unbalanced grid," *IET Power Electron.*, vol. 7, no. 1, pp. 41–49, Jan. 2014.
[23] M. Hamouda, H. F. Blanchette, and K. Al-Haddad, "Unity power factor operation of indirect matrix converter tied to unbalanced grid," *IEEE Trans. Power Electron.*, vol. 31, no. 2, pp. 1095–1107, Feb. 2016.

**Grzegorz Iwanski** (Senior Member, IEEE) received the M.Sc. degree in automatic control and robotics and the Ph.D. degree in electrical engineering from the Faculty of Electrical Engineering, Warsaw University of Technology (WUT), Warsaw, Poland, in 2003 and 2005, respectively.

From January 2006 to December 2008, he was a Research Worker involved in an international project within the Sixth Framework Programme of the European Union (EU). Since 2009, he has been an Assistant Professor with the Institute of Control and Industrial Electronics, WUT, where he became an Associate Professor in 2019. In 2012/2013, he joined the Renewable Electrical Energy System (REES) Team, Universitat Politècnica de Catalunya (UPC), Barcelona, Terrassa, Spain, within the framework of the scholarship of Polish Minister of Science and Higher Education. He is a coauthor of one monograph, three book chapters, and about 70 journal articles and conference papers. He teaches courses on power electronics, drives, and power conversion systems. His research interests include variable and adjustable speed power generation systems, photovoltaic and energy storage systems, and automotive power electronics and drives.

Dr. Iwanski provided two plenary lectures on IEEE technically sponsored international conferences: Ecological Vehicles and Renewable Energies (EVER'15) and Joint International Conference on Optimization of Electrical and Electronic Equipment and Aegean Conference on Electrical Machines and Power (OPTIM-ACEMP'17).

**Paweł Maciejewski** received the M.Sc. degree in automatic control and robotics and the Ph.D. degree in electrical engineering from the Faculty of Electrical Engineering, Warsaw University of Technology (WUT), Warsaw, Poland, in 2012 and 2019, respectively.

Since 2018, he has been an Assistant Professor with the Institute of Control and Industrial Electronics, WUT. He teaches courses on electric drives and energy conversion systems. His research interests include electric drives and generating systems with induction machines.

**Tomasz Łuszczyk** received the M.Sc. and Ph.D. degrees in electrical engineering from the Faculty of Electrical Engineering, Warsaw University of Technology (WUT), Warsaw, Poland, in 2011 and 2017, respectively.

Since 2017, he has been an Assistant Professor with the Institute of Control and Industrial Electronics, WUT. His research is concentrated on vector control of electric machines and grid converters.